PERGAMON

International Journal of Heat and Mass Transfer 43 (2000) 1053–1066

International Journal of HEAT and MASS TRANSFER

www.elsevier.com/locate/ijhmt

Phasewise numerical integration of finite element method applied to solidification processes

N. Nigro*, A. Huespe, V. Fachinotti

Grupo de Tecnología Mecánica del INTEC, CONICET — Universidad Nacional del Litoral, Güemes 3450, 3000 Santa Fe, Argentina

Received 3 December 1998; received in revised form 25 June 1999

Abstract

Phase change is a very complex physical phenomenon that governs a lot of industrial situations. Due to the inherent difficulties that arise in manufacturing activities they need a numerical treatment using models to predict the behavior of the different phases involved in the process. Historically, solidification problems were solved considering only the solution of an energy balance with isothermal phase change including conduction and or convection in the material. Nowadays computational fluid dynamics is becoming a well-suited numerical technique to investigate all kind of transport phenomena, especially when coupled fields are involved. This trend has addressed the research in solidification problems towards the solution of models combining incompressible Navier–Stokes equations coupled with heat and mass transfer including phase change. In this paper we present a phasewise discontinuous numerical integration method to solve thermal phase change problems in a fast and accurate way. Moreover, this methodology was extended to coupled fluid flow and energy balance equations with success and in a future work we will apply to binary alloy solidification with macrosegregation.

Keywords: Solidification; Phase change; FEM

1. Introduction

The computational modeling in metallurgical process is becoming more and more attractive during the last decade mainly because the difficulties to make observations of fluid flow inside molds, the fact that the molds and the molten metal are opaque, the temperatures are very high and the conditions are highly transient and risky. Therefore, computational fluid dynamics (CFD) is usually the most economical and practical way to get information about what is going on inside a casting device and it is often the only feasible way. Besides these technical and economical reasons there are some others related with the mathematical complexity to treat industrial scale solidification problems. Absorption or release of latent heat makes phase change problems nonlinear and exact solutions are only restricted to few problems involving pure substances in very simple domains. The inability of these solutions to address multidimensional effects, non-discrete or non-isothermal phase change, advection dominated situations, has moved the attention towards numerical procedures. In thermal phase change problems it is very popular to divide the numerical methods in two main methodologies: *multiple region* or *variable grid methods*, where independent conservation equations for each phase are formulated

* Corresponding author. Tel.: +54-42-559174; fax: +54-42-550944.

E-mail address: nnigro@intec.unl.edu.ar (N. Nigro).

0017-9310/00/$ - see front matter
PII: S0017-9310(99)00220-3

Nomenclature

C_p specific heat capacity
c solute concentration
f mass fraction
$\boldsymbol{g}$ gravity acceleration
h grid size
$\boldsymbol{I}$ second order identity tensor
$\boldsymbol{K}_p$ permeability tensor
k_p partition coefficient
$\mathscr{L}$ specific latent heat
m_l slope of the liquidus line
p pressure
Ste Stefan number
T temperature
t time
T_m melting point of pure metal
U_{in} pouring velocity (continuous casting problem)
$\boldsymbol{u}$ velocity

Greek symbols
$\Delta\beta$ volumetric expansion coefficient
$\boldsymbol{\epsilon}$ strain rate tensor
κ thermal conductivity
ρ density
$\boldsymbol{\sigma}$ stress tensor
μ dynamic viscosity

Subscripts
∞ reference value
l liquid phase
s solid phase
T transpose

and they are coupled by boundary conditions at the interface, and *single region* or *fixed grid formulation* that are generally developed from volume-averaged techniques based on classical mixture theory or by a continuum formulation. They eliminate the need for separate phase conservation equations producing one phase form models for the mixture. In the solidification of industrial alloy the several different substances are generally added to improve the quality of the cast yield. This multicomponent mixture promotes a phase change that covers a temperature range with a behavior that depends on phase change environment, composition and thermodynamic descriptions of specific phase transformation. Assuming no phase transition in the solidification process we focus only on liquid–solid phase change occurring in a region called *mushy zone* where both phases are present. This zone is often formed by solid dendrites and interdendritic liquid that separates the fully solidified and melted regions as a permeable crystalline-like matrix coexisting with the liquid phase. Dendrites grow naturally due to a nucleation mechanism with an inherent scale of the order of 10 μm and with a highly irregular morphology. This fact makes the single domain techniques more attractive. Early attempts to treat conduction phase change problems using continuum formulation have shown to be successful. Bennon and Incropera [1] have extended its application to advection dominated flows coupling momentum, heat and species transfer in binary alloy, starting a very interesting scientific discussion about mathematical modeling of these phenomena. Considerations about multiphase region morphology and relative phase velocities were addressed in this paper. Others single domain models of binary solidification have presented in recent years. Voller and Prakash [2] and Voller et al. [3,4] have used this formulation for coupling momentum, energy and mass transfer in solidification problems. They have focused their attention in different ways to model the interface interaction assuming different morphology for solid and liquid phases. Beckermann and Viskanta [5] chose to cite volume-averaging literature instead of mixture literature as a justification for the conservation equations associated with individual phases. Ganesan and Poirier [6] have begun a fruitful discussion since they stated that both approaches, volume-averaged and continuum formulation, were quite different. Prescott et al. [7] have demonstrated that the two models yield essentially equivalent results. While continuum formulation is questionable by the way in which phase interactions source terms appear, also it should be mentioned that volume-averaged approach needs some additional information to be supplied concerning with the treatment of mathematical operators applied to volume-averaged quantities. Other explicit goal of continuum formulation is that related to put the conservation equations in a single-phase (mixture) form adding source terms to arrive to the right balance equations. This methodology makes continuum formulation very suitable to be solved by standard CFD codes and to clarify the physical meaning of the different terms. On the other hand the volume-averaged approach generally arrives to a momentum transfer equation expressed in terms of liquid phase velocity instead of mixture velocity. Moreover, the dominant physical mechanisms governing fluid flow in the mushy

zone are quite different from those belonging to the whole liquid region, so the continuum formulation needs some criteria for neglecting or retaining terms according to the phase involved. In this work a special numerical integration method based on temperature model is introduced in order to avoid some of the difficulties introduced by the discontinuities presented in most of the fixed grid phase change formulations. In this way it is possible to get the exact Jacobian matrix of the Newton scheme retaining the quadratic convergence rate. This strategy was extended to include the solution of thermally coupled fluid flow with phase change and it has shown to be very efficient in several tests. Another important remark is about the robustness of this strategy to solve not only mushy phase change, also almost isothermal phase change problems. This idea was originally presented as a discontinuous integration scheme by Steven [8] to solve Poisson equation with discontinuous coefficients and lately by Crivelli et al. [9] and Storti [10] for isothermal phase change problems. In recent papers Fachinotti et al. [11,12] have adopted this technique to solve the conductive and/or convective heat equation with isothermal or mushy phase change, oriented to continuous casting processes. In these last two papers the authors have adopted an exact integration scheme only over the phase change terms. We emphasize that the central contribution of this paper is around the phasewise numerical integration to solve incompressible Navier–Stokes equations augmented by mushy or almost isothermal phase change equation in a monolithic way. The layout of this paper is as follows: Section 2 introduces the mathematical model used for the solidification process. Section 3 deals with the numerical discretization of the problem and the following shows particularly details about the phasewise numerical integration method. Finally numerical results and conclusions are presented.

2. Mathematical modeling

The conservation equations have been derived on the basis of a continuum model for binary alloy [1]. In the continuum model classical mixture theory is used to develop the governing equations for the entire domain. The unknown variables of these single-phase models are usually the mixture properties.

2.1. Conservation equations

Taking the same assumptions as in the paper of Bennon and Incropera [1] we arrive to the following set of conservation equations:

Mass conservation

$$\frac{\partial}{\partial t}\rho + \nabla\cdot(\rho\boldsymbol{u}) = 0 \tag{1}$$

Momentum conservation

$$\rho\left(\frac{\partial \boldsymbol{u}}{\partial t} + \boldsymbol{u}\cdot\nabla\boldsymbol{u}\right) - \nabla\cdot\boldsymbol{\sigma} = -\rho\boldsymbol{g}\Delta\beta_{\mathrm{T}}(T-T_\infty) - \rho\boldsymbol{g}\Delta\beta_{\mathrm{C}}(c-c_\infty) - \mu_{\mathrm{l}}\mathbf{K}_{\mathrm{p}}^{-1}(\boldsymbol{u}-\boldsymbol{u}_{\mathrm{s}})$$

$$\boldsymbol{\sigma} = -p\mathbf{I} + 2\mu\boldsymbol{\epsilon}(\boldsymbol{u}), \quad \boldsymbol{\epsilon}(\boldsymbol{u}) = \frac{1}{2}\left(\nabla\boldsymbol{u} + (\nabla\boldsymbol{u})^{\mathrm{T}}\right)$$

$$\mu = f_{\mathrm{s}}\mu_{\mathrm{s}} + f_{\mathrm{l}}\mu_{\mathrm{l}} \tag{2}$$

having considered equal density values for both solid and liquid phases and the following assumptions:

1. there are only two phases, liquid and solid,
2. constant phase densities,
3. solid matrix is free of internal stress,
4. solid matrix translates at a prescribed velocity $\boldsymbol{u}_{\mathrm{s}}$,
5. viscous stress from local density gradients are negligible $\nabla(\frac{\rho}{\rho_{\mathrm{l}}}) = 0$,
6. the fluid is assumed to behave as Newtonian with μ as the dynamic viscosity.

Even though the turbulence plays a central role in the definition of transport properties here we neglects its influence assuming a laminar viscosity for the liquid phase μ_{l}. The material solidification that takes place within the mushy zone produces a decrement of the mixture velocity. This effect may be modeled assuming an augmented viscosity for the solid phase or treating the mushy region as a porous medium. While in the former case the solid phase viscosity is enlarged by a factor f_{mushy} relative to the liquid viscosity, in the latter one the morphology of the mushy region is characterized by a permeability tensor $\boldsymbol{K}_{\mathrm{p}}$ obtained by experimental evidences. Even though the incompressibility hypothesis does not allow density variations, these may be incorporated as buoyancy forces in the momentum equations. In this work the Boussinesq linear theory is used to account for the contraction and the expansion of the material due to local thermal and solutal gradients. In Eq. (2) $\Delta\beta_{\mathrm{T}}$ and $\Delta\beta_{\mathrm{C}}$ represent the thermal and solutal volumetric expansion coefficients and T_∞, c_∞ represent the temperature and the solutal concentration reference values used for the constant density computation.

Energy conservation

$$\frac{\partial}{\partial t}T + \nabla\cdot(\boldsymbol{u}T) = \nabla\cdot\left(\frac{\kappa}{\rho C_{\mathrm{p}}}\nabla T\right) - \frac{\mathscr{L}}{C_p}\left(\frac{\partial}{\partial t}f_{\mathrm{l}} + \nabla\cdot(\boldsymbol{u}_{\mathrm{s}}f_{\mathrm{l}})\right)$$

$$\kappa = f_{\mathrm{s}}\kappa_{\mathrm{s}} + f_{\mathrm{l}}\kappa_{\mathrm{l}}, \tag{3}$$

where, for simplicity, we have assumed that both phases have the same density and specific heat ($\rho_{\mathrm{s}} = \rho_{\mathrm{l}} = \rho$, $C_{\mathrm{p_s}} = C_{\mathrm{p_l}} = C_{\mathrm{p}}$) with constant values. Also we have used the assumption of saturated systems ($f_{\mathrm{s}} + f_{\mathrm{l}} = 1$) with κ representing the mixture conductivity.

2.2. Closure equations

In order to complete the mathematical model it is necessary to introduce the closure equations.

2.2.1. Thermodynamic equilibrium at interface

First, we need some relationships between temperature and concentration given by experimental evidences. In binary systems it is very common to use a thermodynamic equilibrium diagram that allows to relate solid and liquid solute concentrations with temperature as:

$$c_{\mathrm{l}} = c_{\mathrm{l}}(T) = \frac{c}{1 + f_{\mathrm{s}}(k_{\mathrm{p}} - 1)}, \quad c_{\mathrm{s}} = c_{\mathrm{s}}(T) = k_{\mathrm{p}}c_{\mathrm{l}}, \quad T_{\mathrm{l}} = T_{\mathrm{m}} + m_{\mathrm{l}}\,c \tag{4}$$

where k_{p} is the partition coefficient, m_{l} is the liquidus line slope and c is the solute concentration in the binary mixture. On the other hand it is necessary to introduce some law for the solid fraction in terms of temperature and concentrations. While lever rule is preferred in those situations with high back diffusion in the solid phase (typical of iron carbon systems), Scheil law may be used in the other extreme situation, where the assumption is no solid phase diffusion with perfect mixing in the liquid phase. In the former case the expression for the liquid fraction is as follows:

$$f_{\mathrm{l}} = 1 - \frac{1}{1 - k_{\mathrm{p}}}\frac{T - T_{\mathrm{l}}}{T - T_{\mathrm{m}}} = 1 - f_{\mathrm{s}} \tag{5}$$

2.2.2. Mushy region treatment

For solving incompressible Navier–Stokes applied to solidification problems, it is necessary to include some numerical strategy to treat the influence of material solidification over the velocity field. Experimental evidences show that the flow in the vicinity of the phase change region is induced to adopt the solid phase velocity. To do this, several authors prefer to choose a very large viscosity value for the solid phase (augmented viscosity) while others prefer to restrict the velocity field assuming that this region is similar to a porous medium, characterized by a permeability tensor. While in the former the solid viscosity is defined as $\mu_{\mathrm{s}} = f_{\mathrm{mushy}}\mu_{\mathrm{l}}$, in the later the definition of the permeability tensor follows the Karman–Kozeny law. In this paper we have adopted an isotropic tensor characterized by

$$\mathbf{K}_{\mathrm{p}} = \frac{f_{\mathrm{l}}^3}{D_1(1 - f_{\mathrm{l}})^2}\boldsymbol{I}, \quad D_1 = \frac{180}{d_{\mathrm{dend}}^2} \tag{6}$$

where $d_{\mathrm{dend}}(\approx 0.01$ m) represents the dendritic secondary arm spacing.

3. Numerical discretization

The incompressible Navier–Stokes equations coupled with energy and species conservation equations with mushy phase change are spatially discretized by finite elements. As it is very well known the incompressibility and advection terms play a crucial role in finding the numerical solution to the mathematical model presented in the above section. The former is responsible for numerical instabilities in the pressure field producing checkerboard modes in the solution that may be avoided using an adequate pair of interpolation functions for velocities and pressure. Historically the CFD scientific community has adopted mixed elements to solve incompressible Navier–Stokes equations at low Reynolds number, needing the usage of some numerical stabilization on the velocity field to achieve reasonable results when using Galerkin method at high Reynolds numbers. During the last decade there is a strong tendency to use equal order interpolation functions with some stabilization in order to circumvent both numerical instabilities, incompressibility modes and advection dominated flows. Among the large amount of stabilized equal order numerical schemes the SUPG-PSPG [13] seems to be very effective, simple and robust and due to these reasons it was adopted for this work. For the energy and species balances we have chosen an SUPG finite element method [14]. In the next sections we describe in more details an efficient and accurate method to solve not only single-phase change problems but also coupled solidification problems.

4. Phasewise numerical integration

As we have mentioned in Section 1, in this paper we present a fast and accurate methodology to solve

mushy phase change problems based on temperature model. This technique was especially designed to treat non-isothermal problems but also it has shown to be very robust to solve a broad range of situations including very thin mushy zone problems. This strategy is classified as a fixed grid method but in some sense it works like a variable grid method adding the contribution of each phase in a separate way. Here we extend this technique using a numerical quadrature integration method well suited to most of the finite element codes and this discontinuous integration is applied to the coupled momentum, heat and mass transfer equations. So, it is possible to use the very attractive features of this technique to solve coupled field problems where material properties could have sharp variations inside those element with more than one phase. In the next section we present details about this strategy applied to thermal problems with mushy phase change. The extension of this methodology to solve coupled incompressible Navier–Stokes equations with thermal phase change, typical model of a lot of industrial casting processes is straightforward.

4.1. The thermal phase change case with conduction and convection

The application of the phasewise discontinuous integration method for the solution of thermal phase change problems consists of dividing the element integration domain in several element subdomains according to the distribution of phases within the element. In this work we have restricted the methodology only to triangular type elements and the extension to tetrahedral elements is straightforward. In each iteration the nodal solid fraction of each element is computed and the corresponding case is detected. Fig. 1 shows one example for each different situation taken into account in this development. In this figure the original triangular element of nodes A, B, C is analyzed according to the number of interfaces crossing through the element domain. The notation [$I\,J\,K$] represents the number of interface-edge intersections at each edge, for example [1 2 0] represents one intersection at the first edge, two at the second and no intersection at the third edge. Two different interfaces cannot intersect an edge at the same point. So, before computing the contribution of each element a special routine identifies the corresponding case according to the nodal solid fraction. To do this it is necessary to compute the intersection coordinates at each triangle edge with the solidus and liquidus line coming from the thermodynamic equilibrium diagram. This is equivalent to map the triangle to this diagram. Then the intersections arise from equalizing the liquidus or solidus line with the edge line. The following step consists of dividing the original triangular domain in several one phase triangular subdomains. At this stage each quadrangle is divided in two triangles and each pentagon is divided in three triangles, so only triangular regions are involved in the numerical integration task. Once the case is identified, the contribution of the original element to the Jacobian matrix and the residual vector is computed as the sum of several contributions, each one coming from single-phase triangular subdomains. Then the thermal residual computation is equivalent to:

$$\boldsymbol{R}_{\mathrm{T}} = \sum_{e=1}^{Ne}\sum_{e'=1}^{Ne'}\int_{\Omega_{e'}(T,\,c)} \tilde{\mathbf{w}}_{\mathrm{T}}\left(-\left(\frac{\partial T}{\partial t} + \boldsymbol{u}\cdot\nabla T\right) + \nabla \cdot\left(\frac{\kappa}{\rho C_p}\nabla T\right) + \frac{\mathscr{L}}{C_p}\left(\frac{\partial f_{\mathrm{s}}}{\partial t} + \boldsymbol{u}_{\mathrm{s}}\cdot\nabla f_{\mathrm{s}}\right)\right) \mathrm{d}\Omega_{e'} \tag{7}$$

with Ne the number of elements in the whole mesh, Ne' the number of triangular subdomains inside each original element, $\tilde{\boldsymbol{w}}_{\mathrm{T}}$ the perturbed weight function of the thermal equation according to SUPG formulation [14] and $\Omega_{e'}$ the triangular subdomain. In order to adapt this computation to standard finite element codes, we need to use only information involving nodes of each triangular subdomain (1, 2,...) and finally add their contributions to the nodes of the original triangular element (A, B, C) (see Fig. 1). To do this we define a variable change between the original coordinates and those belonging to each triangular subdomain. Let $\boldsymbol{X} = [x, y]$ be a given point interior to the original element and belonging to only one of the subdomains shown in Fig. 1. This point may be placed in terms of the original shape functions $\mathbf{w}$ or in terms of those corresponding to the subdomain just mentioned $\boldsymbol{w}^*$. So,

$$x = w_i x_i = \boldsymbol{w}^{\mathrm{T}}\begin{pmatrix} x_A \\ x_B \\ x_C \end{pmatrix} = w_i^* x_i^* = \boldsymbol{w}^{*\mathrm{T}}\begin{pmatrix} x_1 \\ x_2 \\ x_3 \end{pmatrix}$$

$$y = w_i y_i = \boldsymbol{w}^{\mathrm{T}}\begin{pmatrix} y_A \\ y_B \\ y_C \end{pmatrix} = w_i^* y_i^* = \boldsymbol{w}^{*\mathrm{T}}\begin{pmatrix} y_1 \\ y_2 \\ y_3 \end{pmatrix}$$

$$\boldsymbol{w} = \begin{pmatrix} w_A \\ w_B \\ w_C \end{pmatrix} \qquad \boldsymbol{w}^* = \begin{pmatrix} w_1 \\ w_2 \\ w_3 \end{pmatrix} \tag{8}$$

$$\boldsymbol{A}\boldsymbol{w} = \boldsymbol{A}^* w^*,$$

$$\mathbf{A} = \begin{pmatrix} 1 & 1 & 1 \\ x_A & x_B & x_C \\ y_A & y_B & y_C \end{pmatrix}, \quad \boldsymbol{A}^* = \begin{pmatrix} 1 & 1 & 1 \\ x_1 & x_2 & x_3 \\ y_1 & y_2 & y_3 \end{pmatrix} \tag{9}$$

where $x_{A,B,C}$ and $x_{1,2,3}$ are the spatial coordinates of

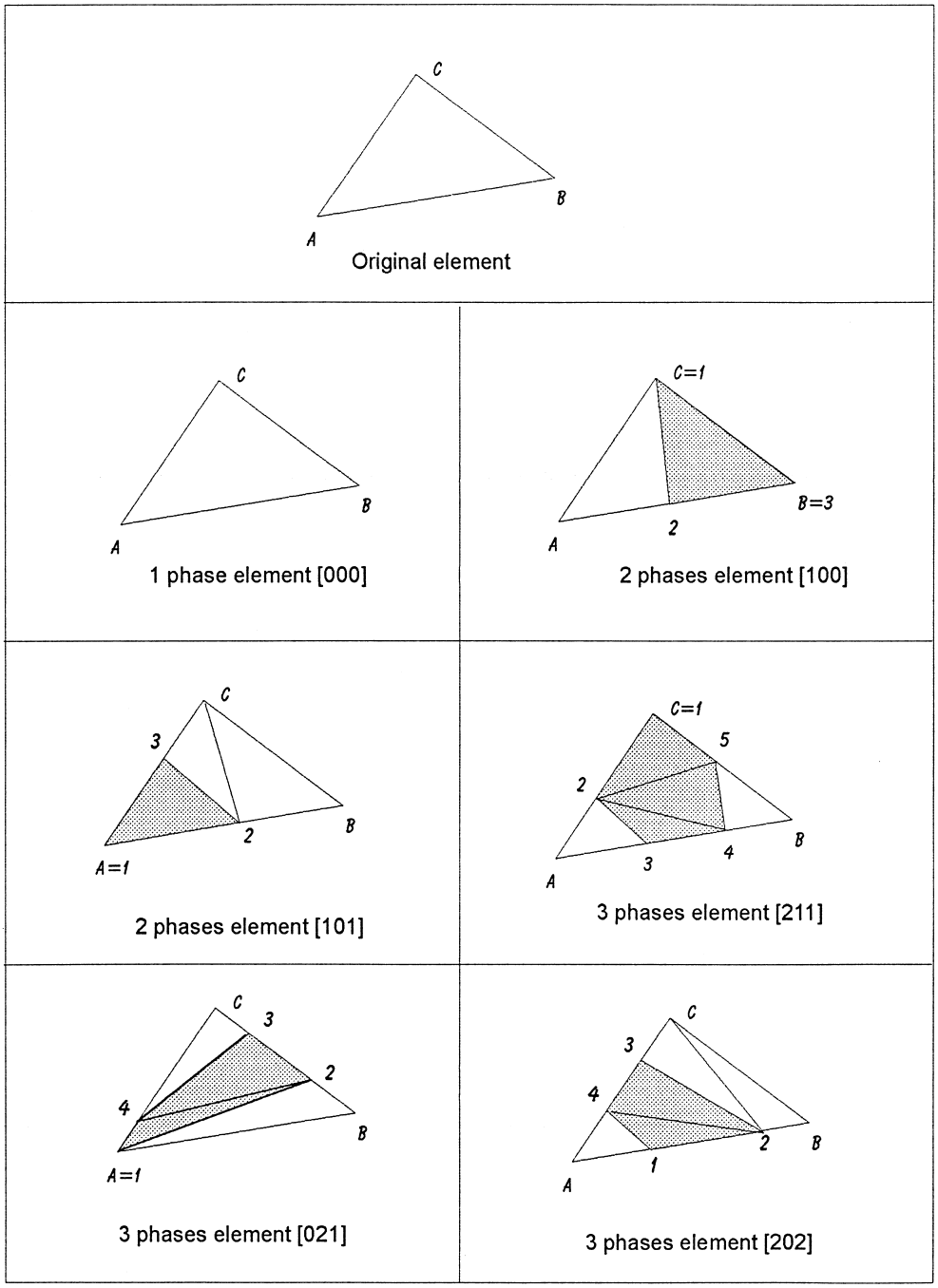

Fig. 1. Phasewise numerical integration method. Identification of possible cases.

both, the original triangle and the triangular subdomain (see Fig. 1). The jacobean matrix is computed as the derivative of the each nodal residue (7) respect to each nodal temperature using also the phasewise strategy and the transformations (8) and (9) presented above.

4.2. Extension to coupled fluid flow and energy balance equations

In order to solve the problem in a monolithic way we adopt for the Navier–Stokes solver a similar strategy as for the energy balance equation. Once the case is identified and the element domain is divided into several triangular subdomains, a phasewise numerical integration is performed using the corresponding single-phase material coefficients regardless of the mathematical continuity of these coefficients.

5. Numerical examples

In this section we present several numerical applications in order to check the efficiency and accuracy of the present method. We start with two unsteady mushy phase change tests, we follow with a continuous casting problem and finally we present a static ingot casting application. The results of these four examples show a good combination of high accuracy with very fast convergence rate being a very good alternative to solve other coupled field phase change problems. All this examples were performed using a standard line-searching and backtracking algorithm to improve the convergence rate.

5.1. Unsteady 1D phase change problem with conduction

The first example is the classic Neumann problem, i.e., the solidification of an initially liquid semi-infinite slab at uniform temperature $T_0 = 0°C$, just above $T_m = -0.1°C$, whose surface temperature suddenly falls to a constant value $T_w = -45°C$. Besides, we assume constant thermo-physical properties: conductivity $\kappa = 1.08$ W/(m K), heat capacity $\rho C_p = 1$ J/(°C m^3) and latent heat $\rho\mathscr{L} = 70.26$ J/m^3. Since an analytical as well as several numerical solutions are available (see Ref. [11]), this problem poses a valuable benchmark for current work. Two meaningful parameters describing the problem are the Stefan number (latent to sensible heat ratio) $Ste = \frac{\rho\mathscr{L}}{\rho c(T_m - T_w)} - T_w = 1.6$, and the dimensionless temperature $T_0^* = \frac{T_0 - T_m}{T_m - T_w} = 2 \times 10^{-3}$. The former governs the temperature gradient discontinuity, while the latter is related to the magnitude of this gradient next to the wall. The solution process performance uses to deteriorate when Ste increases or T_0^* decreases [15]. The above-mentioned values lead to a critical circumstance wherein enthalpy models fail to converge, unless a large fictitious regularization range were introduced against the isothermal character of the problem, as demonstrated by Celentano [16]. So, this example is useful to remark the convergence ability of the present method. For this particular application the space-time discretization was $h = 0.125$ m and $\Delta t = 0.1$ s.

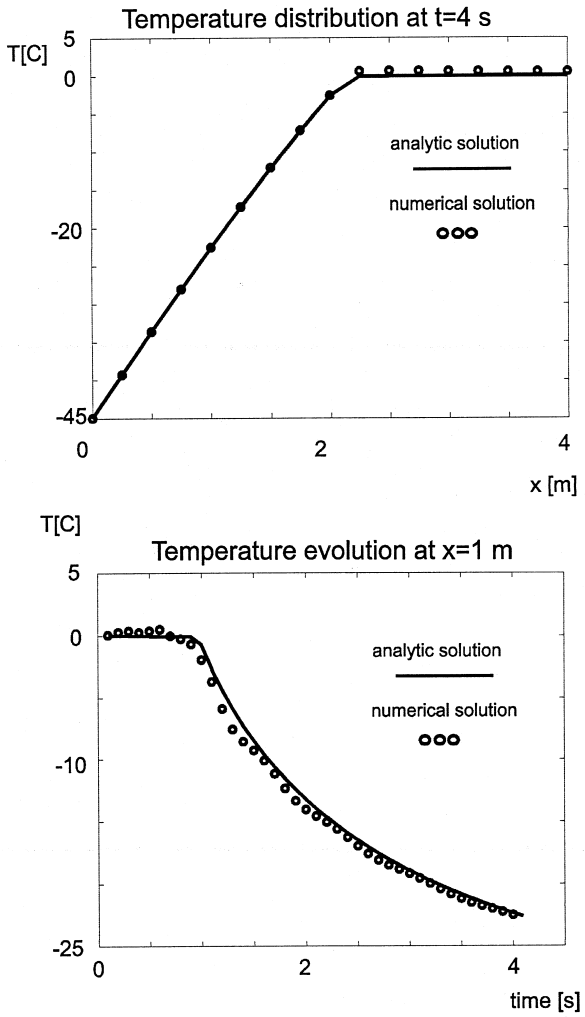

Fig. 2. Unsteady 1-D phase change problem with conduction.

The current model closely represents the exact response, as it is shown in Fig. 2 for the temperature field in the upper plot (at $t = 4$ s) and the thermal history (at $x = 1$ m) in the lower one. Using only one time step computation $\Delta t = t = 4$ s the residual norm decays quadratically and after eight iterations the convergence is attained ($\|R\| < 10^{-12}$). On the other hand, for $\Delta t = t/40 = 0.1$ s the convergence in each time step is reached in a few iterations, varying from a maximum of 13 iterations to a minimum of 5 iterations.

5.2. Unsteady planar 2-D nearly isothermal phase change problem with conduction

The second test offers technological interest. It consists of a steel ingot in a mold during early stages of solidification [11,16]. Its transverse section will be considered, just a quarter of which will be modeled

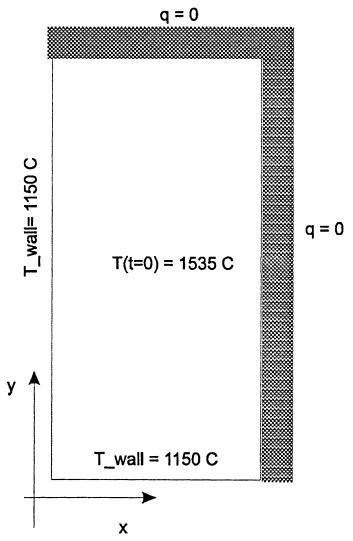

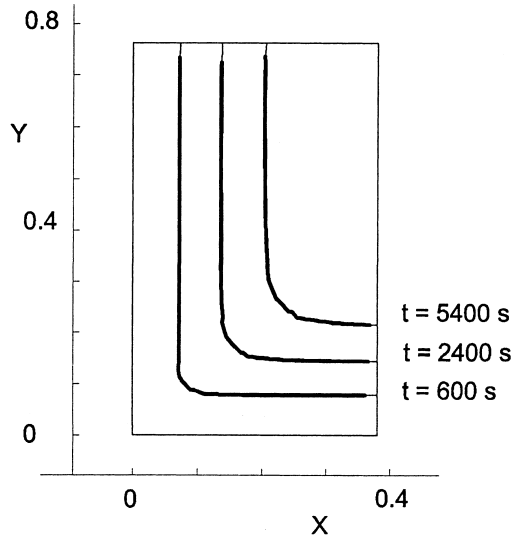

Fig. 3. Unsteady planar 2-D nearly isothermal phase change problem with conduction. Geometry, boundary conditions and advance of solidification front.

because of symmetry conditions (Fig. 3). We assume a nearly isothermal process ($T_m = 1500°C$) with constant thermo-physical properties: $\kappa = 30$ W/(m K), $\rho C_p = 5.4 \times 10^3$ kJ/(°C m^3), $\rho \mathscr{L} = 1.89 \times 10^6$ kJ/m^3. Since $Ste = 1$ and $T_0^* = 0.1$, it seems to be in a more favorable situation than the previous example. Rathjen and Jiji [17] have proposed an analytical solution by similarity transformation for a semiinfinite corner region, usually taken as a reference for the current problem. The geometry, boundary conditions and the front advance with time for a time step of $\Delta t = t/10$ are shown in Fig. 3. This solution and another using $\Delta t = t$ are in good agreement with the semi-analytical expression. Fig. 4 shows both numerical and semi-analytical solutions for the temperature distribution along the bisecting line $x = y$ at three different instants: $t =$ 600 s (upper), 2400 s (middle) and 5400 s (lower). The accuracy of this model to predict the interface location is as high as expected, no matter how refined the time and space domains are, as it was clearly seen in several numerical experiments cited on [11]. The performance of the numerical solution process is outstanding. Convergence is achieved in a few iterations, typically 20, when using only one time step to reach the final time, pointing out the efficiency of the present tangent scheme. About 10 iterations at each time step was spent when $\Delta t = t/10$ showing a very fast convergence rate for unsteady phase change simulations.

5.3. Steady 2-D axisymmetric mushy phase change problem with convection (continuous casting problem)

The third example is devoted to the numerical simulation of a round billet obtained by continuous casting processing. The problem is described in the upper plot of Fig. 5. The liquid metal is poured into an open mould through a nozzle. This water-cooled mould extracts enough heat from the liquid, solidifying an external thin shell, which is capable of containing the melt inside. Fig. 5 shows on the upper left the main geometrical parameters, at the primary cooling zone the molten metal is poured through a nozzle of r_s radius and suddenly the flow is expanded filling the whole mould diameter D_m. At the wall the strand is in contact with a cooper mould cooled by counterflow water, whose length is L_m. Several water sprays, followed by rolling until the complete section solidifies represent the secondary cooling zone. This process is considered stationary. On the left plot the shading area corresponds to the simulated length (L_s). On the right we have included the main boundary conditions of this problem, where at the inlet nozzle temperature is fixed to $T_{in} = 1530°C$ and at the meniscus, centerline and at the outlet the normal derivative of temperature is negligible. At the mould wall we have assumed a heat flow removal given by a heat flux law similar to Savage–Pritchard

$$\mathbf{q}_s[\mathrm{W/m^2}] = A - B\sqrt{\frac{z}{U_0}} + Cz + \mathrm{d}z^2 \tag{10}$$

with z [m] the axial coordinate and $\mathbf{u}_s = U_0 = 0.03$ [m/s] the casting velocity. We have used the following constant values: $A = 2.1974 \times 10^6$, $C = 3.3737 \times 10^6$, $B = 5.6467 \times 10^5$, $D = 0.16054 \times 10^6$, adjusted by experimental measurements to take into account the air

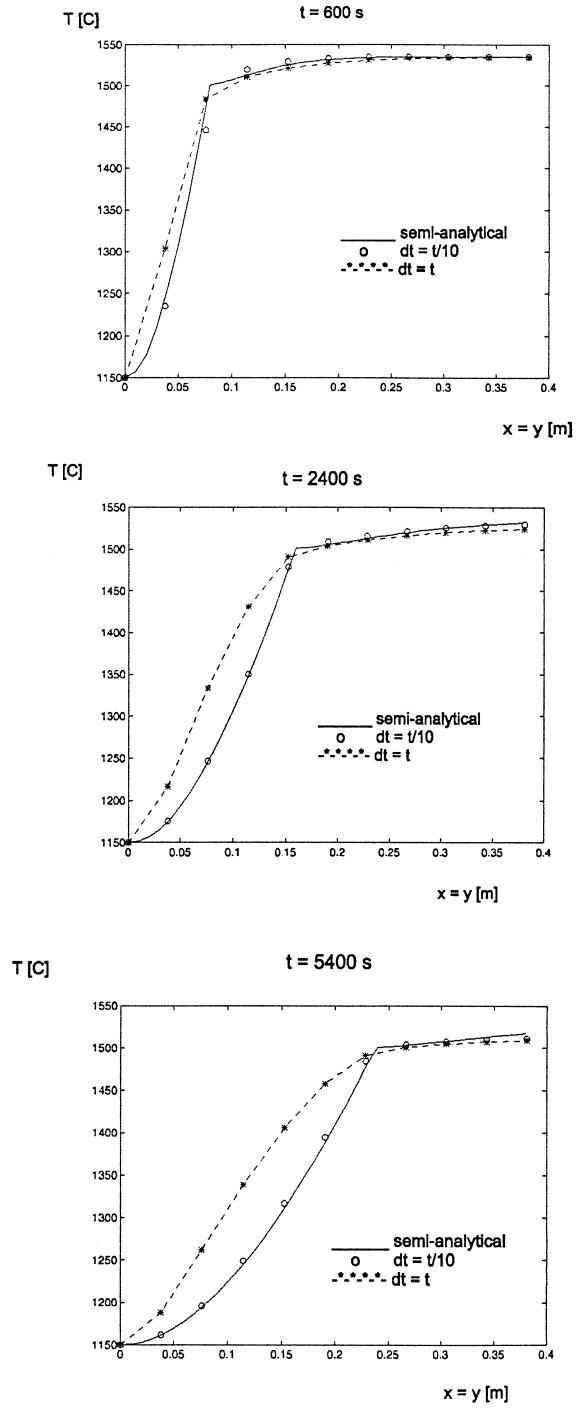

Fig. 4. Unsteady 2-D planar nearly isothermal phase change problem with conduction. Temperature along the bisecting line at (a) $t = 600$ s, (b) 2400 s and (c) 5400 s.

gap formation in this zone. At the water sprays a convective boundary condition is imposed, with a film coefficient h_{spray} and a water external temperature of T_{amb}. Particularly, the material consists of a 0.3 wt% carbon content steel, with the following properties: $\rho = 7200$ kg/m^3, $\kappa_l = \kappa_s = 34$ W/(m K), $C_p = 680$ J/(kg K), $\mathscr{L} = 272{,}000$ J/kg, $T_s = 1455$°C, $T_l = 1493$°C, $T_m = 1537$°C, $h_{\text{spray}} = 500$ W/(m^2 K) and $T_{\text{amb}} = 40$°C The following geometrical data were used: $U_{\text{in}} = 0.8895$ m/s, $D_m = 2 \times 0.106$ m, $r_s = 0.02$ m, $L_m = 0.6$ m and $L_s = 1.5$ m.

Thermal conductivity, density and heat capacity are assumed constant for the current application. The domain of analysis is extended from the top until a small distance below the mould, as it is shown by the shading area in Fig. 5. Let us remark that the complete solidification of the billet is expected to occur at a distance greater than 10 m from the bottom of the mould. We use a structured mesh of 4536 triangles, 2368 nodes. It is denser at the contour, especially next to the mould. The computed temperature field using the SUPG formulation is depicted as isocurves in lower plot of Fig. 5. Fig. 6 plots at the upper part the axial distribution of temperature at external radius, just lying on the mould wall and the water sprays. Maximum differences of 5°C between this techniques and an standard method [18] were found. Lower plot of Fig. 6 shows the convergence rate for the standard code (named old) and the new methodology presented in this paper. In less than 10 iterations the residual has decreased more than 10 orders of magnitude while the old version demands more than 100 iterations. These results are in very good agreement with those obtained by Fachinotti et al. [11] using an exact integration scheme. For solving this problem the fixed velocity field was obtained previously by solving the incompressible Navier–Stokes equations with fixed temperature and concentration. The boundary conditions for the inlet and outlet velocities combined with the casting speed $\mathbf{u}_s = U_0$ satisfied the mass balance. This velocity field is kept frozen during the temperature computation.

5.4. Unsteady Navier–Stokes equations coupled with mushy phase change problem

This test problem, proposed by Voller and Prakash [2], consists of freezing an initially liquid material in a thermal square cavity of size (1×1) under natural convection. Initially the cavity is completely filled with liquid material at $T_0 = T_h = 0.5 > T_l = 0.1$ and the temperature of the left wall is decreased to $T_c = -0.5 < T_s = -0.1$, keeping insulated the top and bottom cavity walls. So, a phase change is set up. While the solidus line shows an almost planar shape the deformation of the liquidus line is more pro-

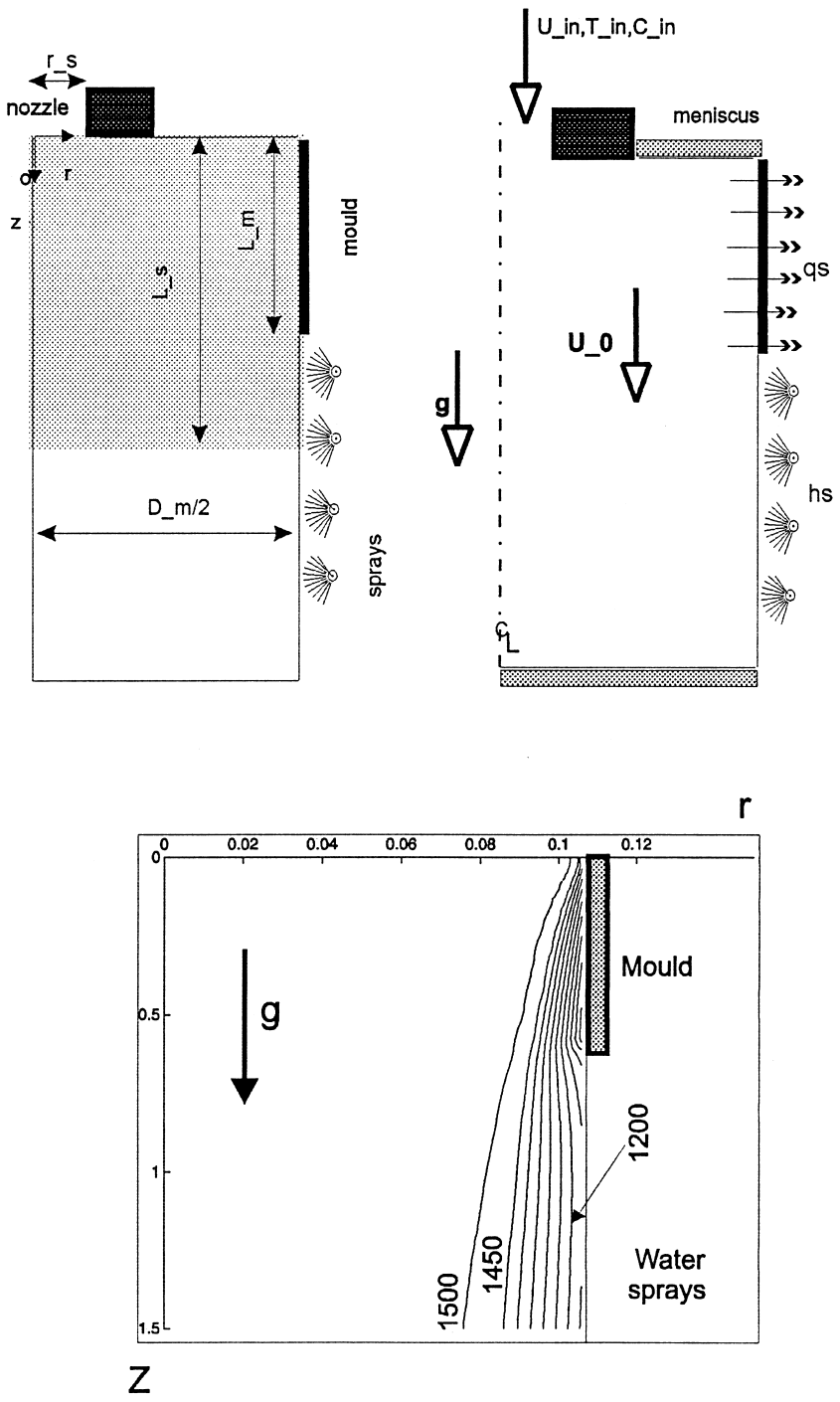

Fig. 5. Continuous casting problem. Geometry, boundary conditions and temperature isocurves.

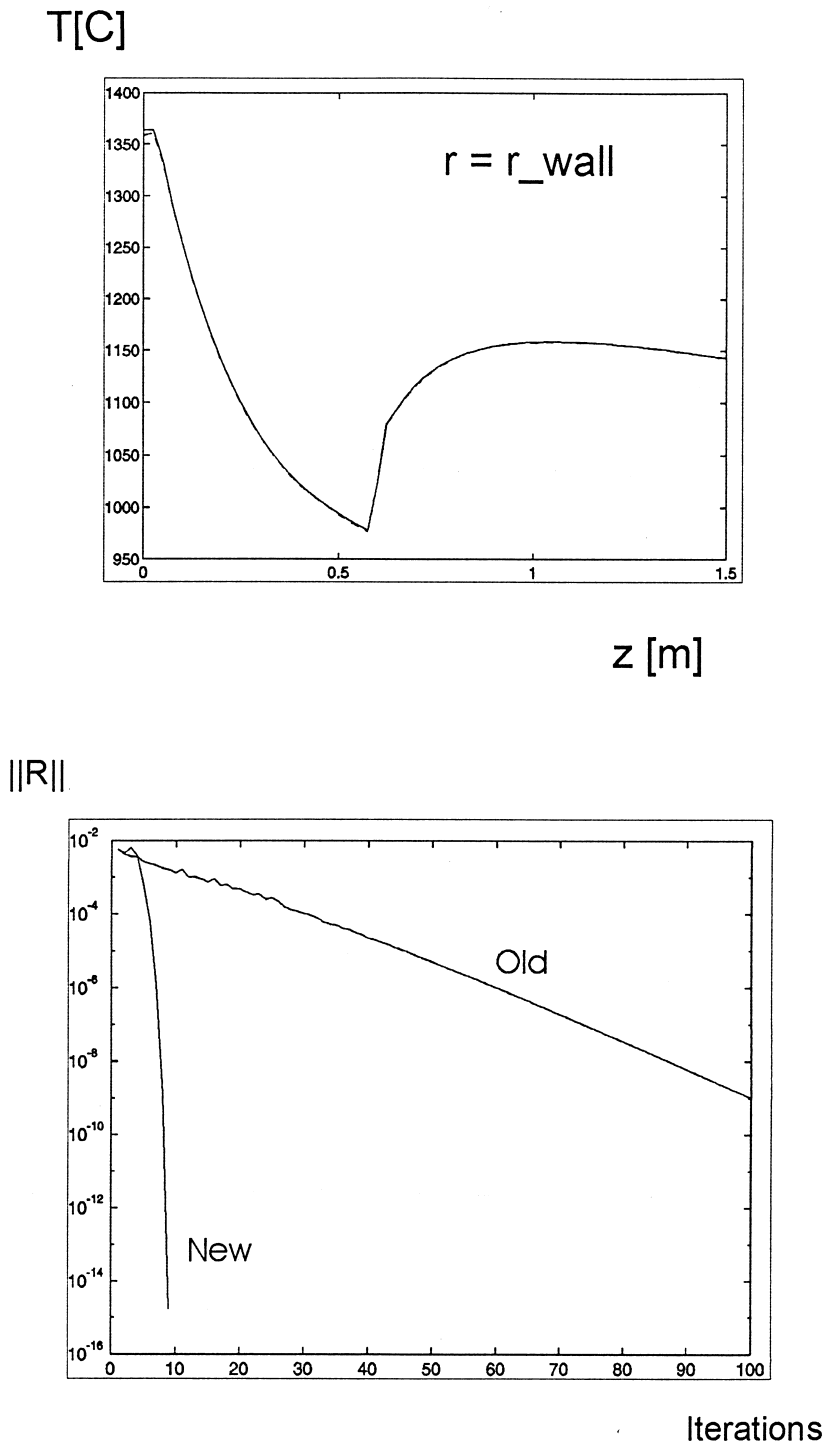

Fig. 6. Continuous casting problem. Temperature at mould wall and convergence rate.

nounced due to convective effects. The thermal gradient promotes the establishment of buoyancy forces in the gravity direction and this phenomenon induces more convection that enhances the deformation, especially in the lower wall making the bulge at the bottom more acute. This example was solved by Voller et al. [2,4] on a set of several grids from 10×10 to 40×40 uniform meshes with a fixed time step of $\Delta t = 10$ s until to a final time of $t = 1000$ s. In that paper the authors reported that in each time step almost 50 iterations were used to solve the discretized equations without under relaxation. They have used a *SIMPLE* algorithm outlined by Patankar [19] implemented on *Phoenics* code. The main parameters were taken from Ref. [2]. The performance of our methodology was successful, with a very fast convergence rate of about five iterations per time step using linesearching and backtracking. In order to study the influence of numerical diffusion and time accuracy we present results for different grid size and time step. Fig. 7 plots the solid liquid interfaces for: (a) $\Delta t = 10$ and $h = 1/40$, (b) $\Delta t = 10$ and $h = 1/20$, (c) $\Delta t = 1$ and $h = 1/40$.

Solidus (S) and liquidus (L) lines at $t = 100$ and 1000 s are shown. There is a noticeable difference between coarse mesh and fine mesh results, but only a little influence of the time step on the interface movement. This remarkable difference may be attributed to the numerical diffusion introduced by the discrete scheme. The liquid front movement tends to a planar advance, typical when the fluid is quiescent due to a viscosity enhancement, being numerical effects one of the main possible reasons. Fig. 8 shows the time evolution of the solid and liquid interfaces at four different times, $t = 100$, 250, and 500 and 1000 s using in this particular case $\Delta t = 10$ and $h = 1/40$. These results are qualitatively in a good agreement with those presented by Voller et al. [4]. Fig. 9 presents the velocity field and the phases distribution at $t = 1000$ s. The three isocurves appearing in the plot represent solid fraction values of $f_s = 0$; 1/2 and 1, being in good agreement with Voller results [4]. More details about the physical meaning of these results may be found in Ref. [2,4]. Here, we are only interested in the comparison of both results with emphasis on accuracy and convergence rate.

6. Conclusions

This paper has presented a numerical integration method based on a phasewise criterion to solve solidification problems coupled with fluid flow. Its efficiency has been proved through several examples. We wish to remark that the discontinuity in the model coefficients is not only a drawback for the heat equation, also for the flow motion. So, the results included in this work confirm the success of this strategy for solidification models that incorporate also the fluid flow. This strat-

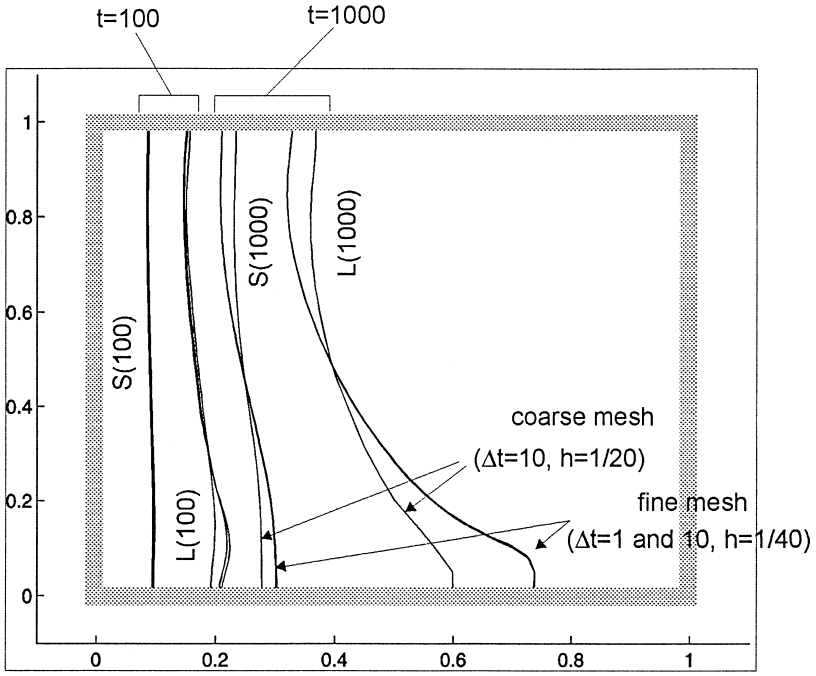

Fig. 7. Unsteady 2D Navier–Stokes equations coupled with mushy phase change problem. Sensitivity with space and time grid size.

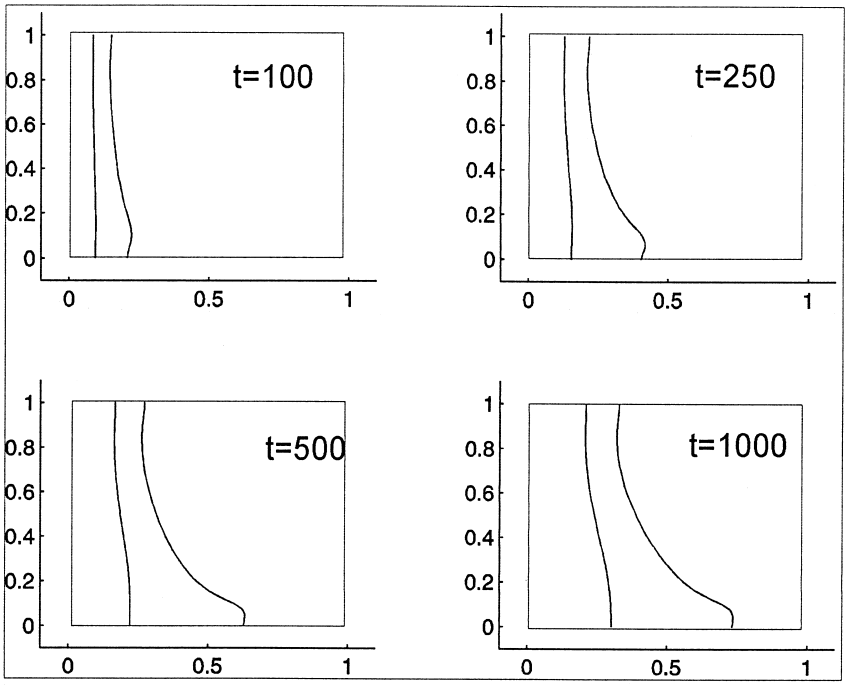

Fig. 8. Unsteady 2D Navier–Stokes equations coupled with mushy phase change problem. Time evolution of solid and liquid interfaces.

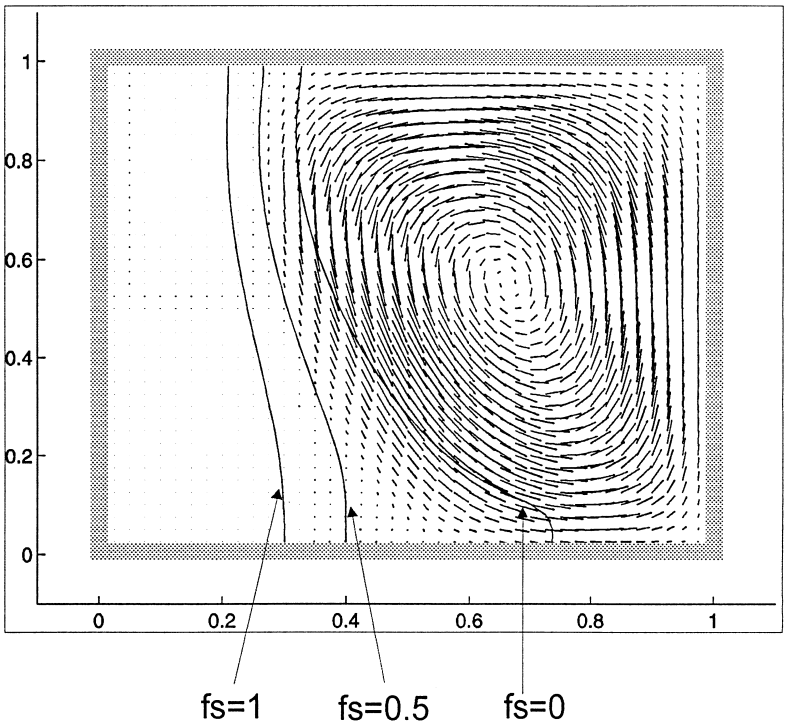

Fig. 9. Unsteady 2D Navier–Stokes equations coupled with mushy phase change problem. Velocity field and phases distribution at $t = 1000$.

egy promises to be an interesting possibility to account for coupled field with mushy or nearly isothermal phase change as in the case of thermomechanical interaction between the mould and the solidified material or in the macrosegregation analysis of casting process.

Acknowledgements

The authors wish to express their gratitude to Consejo Nacional de Investigaciones Científicas y Técnicas (CONICET, Argentina) for its financial support.

References

[1] W. Bennon, F. Incropera, A continuum model for momentum, heat and species transport in binary solid–liquid phase change systems—I. Model formulation, Int. J. Heat Mass Transfer 30 (10) (1987) 2161–2170.
[2] V. Voller, C. Prakash, A fixed grid numerical modeling methodology for convection–diffusion mushy region phase change problems, Int. J. Heat Mass Transfer 30 (8) (1987) 1709–1719.
[3] V. Voller, A. Brent, C. Prakash, The modeling of heat, mass and solute transport in solification systems, Int. J. Heat Mass Transfer 32 (9) (1989) 1719–1731.
[4] V. Voller, A. Brent, C. Prakash, Modeling the mushy region in a binary alloy, Applied Math. Modeling 14 (1990) 320–326.
[5] C. Beckermann, R. Viskanta, Double diffusive convection during dendritic solidification of a binary mixture, PhysicoChem Hydrodyn 10 (1988) 195–213.
[6] S. Ganesan, D. Poirier, Conservation of mass and momentum for the flow of finterdendritic liquid during solidification, Metallurgical Transactions B 21B (1990) 173–181.
[7] P. Prescott, F. Incropera, W. Bennon, Modeling of dendritic solidification systems: reassessment of the continuum momentum equation, Int. J. Heat Mass Transfer 34 (9) (1991) 2351–2359.
[8] G. Steven, Internally discontinuous finite elements for moving interface problems, Int. J. Numer. Methods Eng 18 (4) (1982) 569–582.
[9] L. Crivelli, S. Idelsohn, A temperature-based finite element solution for phase change problems, Int. J. Numer. Methods Eng 23 (1986) 99–119.
[10] M. Storti, Modelación numérica de problemas de frontera libre y móvil, Ph.D. Thesis, Universidad Nacional del Litoral, Santa Fe, Argentina, 1990.
[11] V. Fachinotti, A. Cardona, A. Huespe, A fast convergent and accurate temperature model for phase change heat conduction, Int. J. Numer. Methods Eng. (1997) (in press).
[12] V. Fachinotti, A. Cardona, A. Huespe, Numerical simulation of conduction–advection problems with phase change, in: VII Congreso Latinoamericano de Transferencia de Calor y Materia, Salta, Argentina, 1998.
[13] T. Tezduyar, S. Mittal, S. Ray, R. Shih, Incompressible flow computations with stabilized bilinear and linear equal order interpolation velocity–pressure elements, Comp. Meth. Applied Mech. Engineering 95 (1992) 221–242.
[14] A. Brooks, T.J.R. Hughes, Streamline Upwind/Petrov-Galerkin formulations for convection dominated flows with particular emphasis on the incompressible Navier–Stokes equations, Comp. Meth. Applied Mech. Engineering 32 (1982) 199–259.
[15] M. Salcudean, Z. Abdullah, On the numerical modeling of heat transfer during solidification processes, Int. J. Numer. Methods Eng 25 (1988) 445–473.
[16] D. Celentano, Un modelo termomecánico para problemas de solidificación de metales, Ph.D. Thesis, Universitat Politècnica de Catalunya, Escola Tècnica Superior d'Enginyers de Camins, Canals i Ports, Barcelona, España, 1994.
[17] K. Rathjen, L. Jiji, Heat conduction with melting ∨
[18] S. Idelsohn, N. Nigro, M. Storti, Segregation in continuous casting processes with coupled solidification and fluid flow modeling, Int. J. Forming Process 1 (2) (1998) 135–162.
[19] S. Patankar, Numerical Heat Transfer and Fluid Flow, Hemisphere, Washington, DC, 1980.